

## Effect of moisture on H<sub>2</sub>S adsorption by copper impregnated activated carbon

Chen-Chia Huang<sup>a,\*</sup>, Chien-Hung Chen<sup>b</sup>, Shu-Min Chu<sup>a</sup>

<sup>a</sup> Department of Chemical Engineering, National Yunlin University of Science and Technology, Douliu, Yunlin 640, Taiwan, ROC

<sup>b</sup> Graduate School of Engineering Science and Technology, National Yunlin University of Science and Technology, Douliu, Yunlin 640, Taiwan, ROC

Received 30 June 2005; received in revised form 1 January 2006; accepted 13 January 2006  
Available online 23 February 2006

### Abstract

The aim of this study is to investigate the effect of moisture on adsorption efficiency of hydrogen sulfide (H<sub>2</sub>S) by impregnated activated carbon (IAC). Copper(II) nitrate was used as an impregnant. Two humidification conditions of IAC, pre-moistened and gas stream containing moisture, were studied. The experimental results revealed that the copper species onto the IAC was suggested to be Cu(OH)<sub>2</sub> that deposited on activated carbon during the impregnation process. The adsorption mechanism of H<sub>2</sub>S by copper impregnated IAC was proposed, involving physic-sorption and chemical reactions. Moreover, the H<sub>2</sub>S breakthrough capacity decreased with increasing the relative humidity of gas stream. The causes were attributed to three points as follow: the competition adsorption occurred between moisture and H<sub>2</sub>S; the copper(II) species reduced to copper(I) species leading to IAC deactivation; and the rate of chemical reaction restrained by moisture.

© 2006 Elsevier B.V. All rights reserved.

**Keywords:** Activated carbon; Impregnation; H<sub>2</sub>S adsorption

### 1. Introduction

Activated carbon (AC) is widely used as an absorbent to remove hydrogen sulfide (H<sub>2</sub>S), due to its high specific surface area and porous structure. H<sub>2</sub>S is an odor gas that causes life threatening at higher concentration (500 ppm). It is well known that H<sub>2</sub>S might be produced from power plants, natural gas, crude oil, and industrial streams [1,2]. Some studies reported [3–5] that the surface properties of carbon (such as pH, functional groups, pore size distribution and specific surface area) correlated with H<sub>2</sub>S removal significantly. Moreover, AC samples involving inorganic impurities (silica, alumina, iron oxide, calcium oxide and magnesia) as catalyst can catalyze H<sub>2</sub>S oxidation and convert to elemental sulfur in the presence of oxygen [6–10]. The presence of moisture in gas stream also plays an important role as a medium to enhance oxidation of H<sub>2</sub>S. The dissolved H<sub>2</sub>S reacts with O<sub>2</sub> and converts

to sulfur species in the water film onto the surface of carbon [8,11,12].

Regeneration of spent AC can be employed using cold/hot water washing or thermal treatment to achieve recycle object, but the H<sub>2</sub>S adsorption capacity after regeneration usually decreased remarkably. The cause is attributed that some sulfur species as elemental sulfur or sulfuric acid is strongly bound with activated sites leading to exhaust irreversibly [13–16].

Furthermore, caustic or acidic impregnated activated carbon (IAC) samples have been employed efficiently to adsorb H<sub>2</sub>S from waste-gas stream [17–22]. Nakamura et al. [21] reported that iron(III) chloride impregnated AC has a high selectivity for H<sub>2</sub>S removal. Chiang et al. [22] used four alkaline materials (such as NaOH, Na<sub>2</sub>CO<sub>3</sub>, KOH and K<sub>2</sub>CO<sub>3</sub>) to impregnate AC, and evaluated their performance for H<sub>2</sub>S adsorption. They found that the performance of IAC for H<sub>2</sub>S adsorption was ranked as NaOH > Na<sub>2</sub>CO<sub>3</sub> > KOH > K<sub>2</sub>CO<sub>3</sub>. Yan et al. [23,24] employed alkaline AC to evaluate adsorption capacity under 1% H<sub>2</sub>S together with moist air (RH = 80%). The results indicated that the capacity of H<sub>2</sub>S on alkaline AC after prehumidification (RH = 100%) was higher than that on alkaline AC without

\* Corresponding author. Tel.: +886 5 534 2601x4616; fax: +886 5 531 2071.  
E-mail address: huangchc@yuntech.edu.tw (C.-C. Huang).

prehumidification. Moreover, McIntyre et al. [25] proposed that whetlerite charcoal impregnated with copper and chromium was aged by moisture, due to the valence of metal transformed.

In this study, we modified AC by copper nitrate reagent and evaluated the H<sub>2</sub>S adsorption capacity onto the same. The objectives of this study were: (1) to determine the adsorption capacity of H<sub>2</sub>S onto Cu-IAC, (2) to discuss the reaction between impregnant and H<sub>2</sub>S, and (3) to investigate the effect of moisture on H<sub>2</sub>S removal by IAC.

## 2. Experiments

### 2.1. Materials

Coconut shell-based AC sample was used as the main porous adsorbents in this study. The fresh AC samples were first immersed with hot water for 2 h to remove impurities prior to the impregnation process. The AC samples were washed several times by de-ionized H<sub>2</sub>O, and then dried in an oven at 378 K for 24 h. The as-prepared AC samples were obtained after above treatment. Copper nitrate, obtained from Showa Chemical Company, 99% purity, was chosen as the impregnant solution.

### 2.2. Impregnation process

The IAC samples were prepared as follows: 30 g of the as-prepared AC samples were immersed in the 150 ml of Cu(NO<sub>3</sub>)<sub>2</sub> solutions with various concentrations (0.05, 0.1 and 0.2 M) and pH values (pH 1, 2 and 3), shook with 100 rpm of rotation rate at 303 K for 24 h. Subsequently, the IAC samples were obtained after filtering and drying at 378 K for 24 h. In this study, the pH value of solution did not be kept constant during impregnation process. The amount of copper deposited onto IAC was determined by an extraction method and measured by an atomic absorption spectroscopy (AA, HITACHI, Z-61100 model).

### 2.3. H<sub>2</sub>S breakthrough capacity measurement

The performance of IAC samples for H<sub>2</sub>S removal was evaluated by the breakthrough capacity test system, as shown in

Fig. 1. The prepared IAC was packed with a fixed height of 2 cm in a stainless steel pipe (inner diameter 2.2 cm, length 20 cm). Both bottom and top sections of IAC packed bed were supported by glass beads. The breakthrough capacity test was performed at 303 K. The certified concentration gas (270 ppmv of H<sub>2</sub>S and helium balance, supplied by the SAN FU Gas Co.) passed through the adsorb-column. The total flow rate was set by 1 L/min. The H<sub>2</sub>S concentration at the outlet of adsorb-column was monitored by a gas chromatograph (GC, China Chromatograph 9800) with flame photometric detector (FPD). All runs were finished as H<sub>2</sub>S effluent concentration reached 270 ppmv.

In this study, the humidification of IAC was conducted by two conditions as follows: (1) the dry IAC adsorbed H<sub>2</sub>S under the relative humidity (RH) of 40–50% or 70–80%. The moisture of gas stream was supplied by using a humidifier. Moreover, the humidity of gas stream was monitored continuously by using a moisture detector (VAISALA, HMP 238). (2) The IAC was pre-moistened in a chamber with RH of 40–50% or 70–80% at 323 K for 24 h prior to dynamic adsorption tests. The gas stream was kept to be dry (RH < 1%) for breakthrough capacity tests packed by the pre-moistened IAC.

### 2.4. Material characterization

The surface potential of AC was measured by a zeta potential analyzer (Brookhaven Instruments, ZetaPlus-Zeta Potential Analyzer 1.23). The potential measurement of AC was performed in the solution with pH ranges from 2 to 7. An X-ray Photoelectron Spectroscopy (XPS, Fison, ESCA210) was used to analyze the copper species loaded onto IAC before and after humidification. The amount of sulfur onto AC after H<sub>2</sub>S adsorption was measured by an elemental analyzer (EA, Elementar Analysensysteme GmbH, Vario EL III). The specific surface area and pore size distribution of AC were determined by a gas adsorption meter (QUANTACHROME, AUTOSORB-1) at 77 K and calculated by using the Brunauer–Emmett–Teller (BET) and the Horvath–Kawazoe (HK) methods, respectively. A thermogravimetric analyzer (TG, CAHN, TG-2121) was employed to thermal analyze AC samples with a heating rate of 2 K/min under air atmosphere.

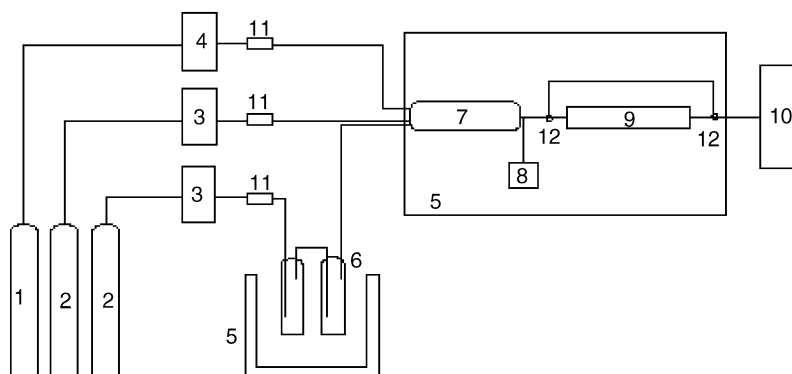


Fig. 1. Schematic diagram of H<sub>2</sub>S dynamic test apparatus. (1) Hydrogen sulfide; (2) helium; (3) mass flow meter; (4) float flow meter; (5) isothermal system; (6) humidifier with water; (7) mixing column; (8) humidity sensor; (9) adsorb-column; (10) GC with FPD; (11) check valve; (12) 3-way valve.

### 3. Results and discussion

#### 3.1. Impregnation process

In this study, copper(II) nitrate was used as an impregnant to modify coconut shell-based AC. The amounts of copper deposited onto AC versus the concentration and pH value of impregnant solution were collected in Table 1. It was found that the pH value of impregnant solution affected significantly the copper species deposition onto the AC. Furthermore, the amount of copper deposition onto the coconut shell-based AC increased with increasing the concentration and pH value of the impregnant solution. In this study, the highest amount of copper deposition was obtained at pH 3 and 0.2 M of impregnant solution.

We also found that the pH value of the impregnant solution was instable during impregnation process. The pH value

Table 1  
Amount of copper deposited onto AC (mmol-Cu/g-AC) under different impregnation conditions

Concentration of copper nitrate (M, mol/L)	pH 1	pH 2	pH 3
0.05	0.0666	0.2212	0.254
0.1	–	–	0.377
0.15	–	–	0.501
0.2	–	–	0.625

of impregnant solution rose immediately when the AC samples immersed into the solution at first time. The surface potential of coconut shell-based AC was revealed to be more negative charge at the higher pH values in range of 2–7 by the zeta potential analysis. According to these results, we proposed the possible impregnation mechanism, as shown in Fig. 2. Copper nitrate dissolved to  $\text{Cu}^{2+}$  and  $\text{NO}_3^-$  ions, which distributed in the as-prepared impregnant solution (step I). When the unmodified AC immersed into the impregnant solution, the negative charge on the surface of AC attracted  $\text{H}^+$  ions in the solution leading to the pH value of solution increasing (step II). Moreover, dissociated copper(II) ions might also be attracted by AC and be associated with hydroxyl ions to form  $\text{Cu}(\text{OH})_2$  (step III). Finally, the  $\text{Cu}(\text{OH})_2$  deposited onto the external-surface and the internal pore of AC (step IV).

#### 3.2. Specific surface area and pore size distribution

The measured specific surface areas of AC and IAC were listed in Table 2. The specific surface area of coconut shell-based AC was  $1050 \text{ m}^2/\text{g}$ . After impregnation process, the specific surface area of IAC decreased to  $789 \text{ m}^2/\text{g}$ . The results suggested that partial pores of AC would be blocked a little due to copper species deposition. Fig. 3 shows the micro-pore distribution of coconut shell-based AC and IAC. It was revealed that the copper species deposited not only onto the meso-pores, but also onto the micro-pores. However, the pore volume of AC slightly decreased after impregnation process.

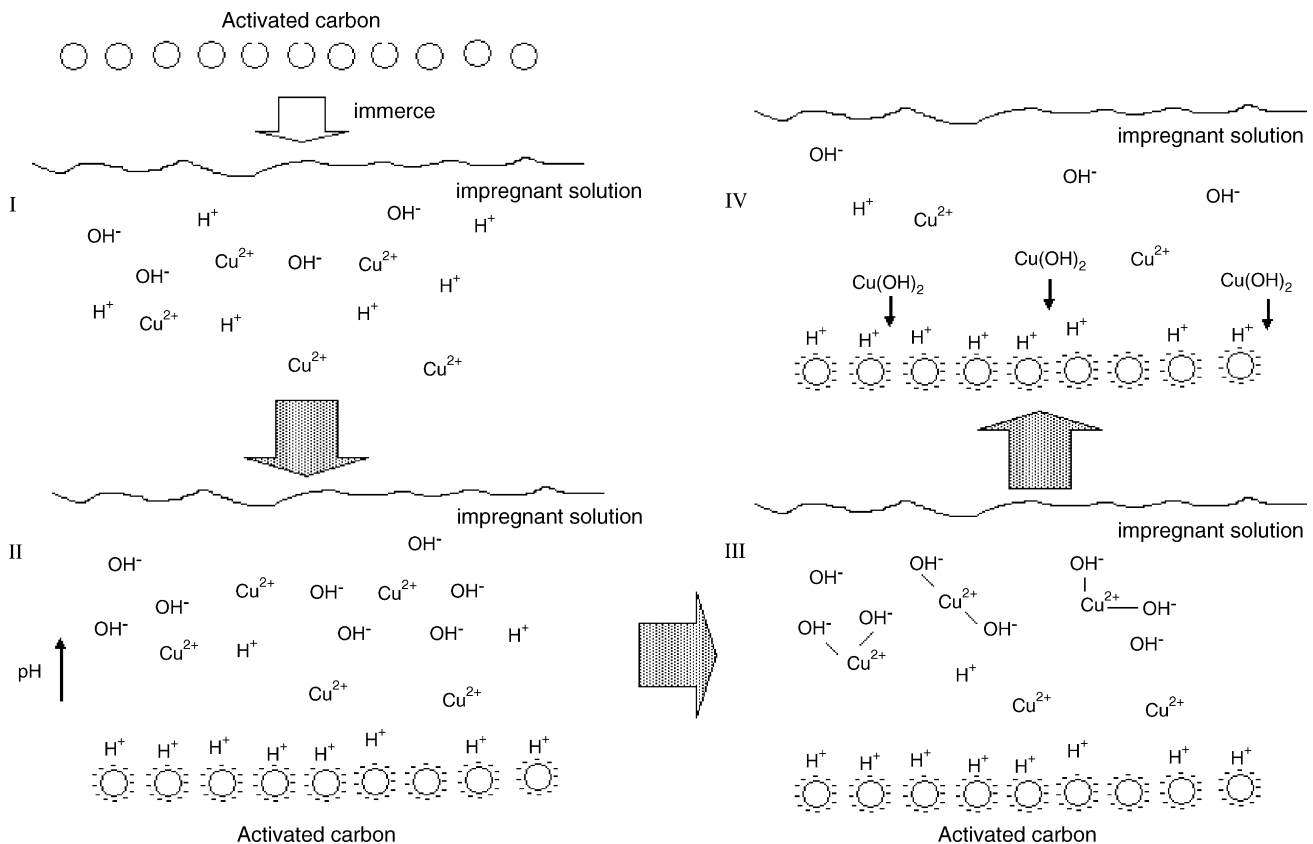


Fig. 2. Schematic representation of impregnation process.

Table 2  
Specific surface area of AC and IAC (impregnant solution: copper nitrate)

Impregnation conditions	Specific surface area (m <sup>2</sup> /g)
Virgin coconut shell-based AC	1050
IAC, pH 3, 0.05 M	856
IAC, pH 3, 0.1 M	864
IAC, pH 3, 0.2 M	789

In other words, the physic-sorption ability of AC was not exhausted.

### 3.3. Thermal analysis

The differential thermogravimetry (DTG) curves of coconut shell-based AC, IAC and IAC after H<sub>2</sub>S adsorption samples were presented in Fig. 4. For IAC after H<sub>2</sub>S adsorption, it was revealed from Fig. 4c that three peaks existed at the temperature range of 373–873 K. The first peak at nearly 373 K was believed to be water vaporization. It was noteworthy that the presence of water from the IAC after H<sub>2</sub>S adsorption sample was apparently higher than that of the other samples. This result confirmed that water was produced during H<sub>2</sub>S adsorption by IAC.

Furthermore, the second peak was observed at 473–493 K, which was considered to be sulfur dioxide evolving. Bagreev et al. [16] developed that sulfur species forms to sulfur dioxide by oxidation at 513 K. The discrepancy of oxidation temperature with preview paper [16] was attributed to the different heating rate. Furthermore, the third peak represented the carbon decomposition. The decomposition temperatures of AC, IAC and IAC after H<sub>2</sub>S adsorption samples were 793, 560 and 640 K, respectively. The results implied that the copper species as catalyst to accelerate the carbon decomposition. Therefore, the decomposition temperature of AC sample decreased after impregnation process. After H<sub>2</sub>S adsorption, however, the decomposition temperature of IAC sample decreased not so much. The cause attributed that copper species onto the AC would be poisoned with H<sub>2</sub>S.

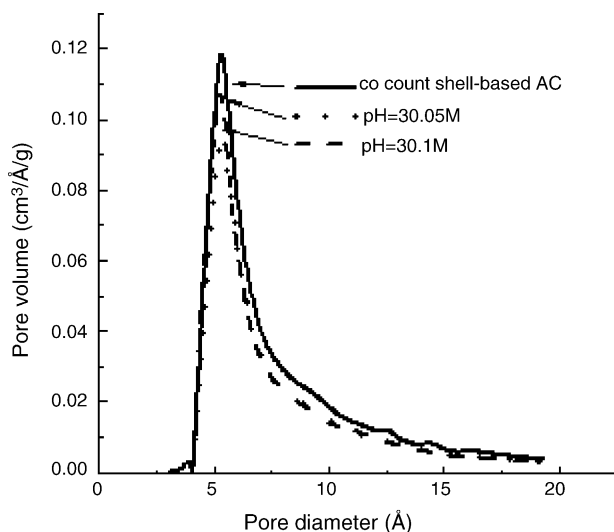


Fig. 3. Pore size distribution of coconut shell-based AC and IAC.

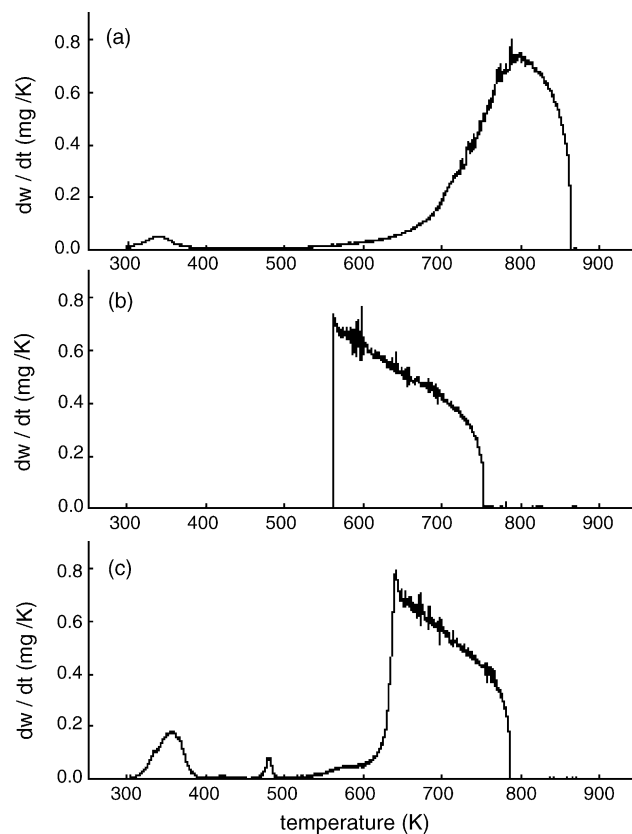
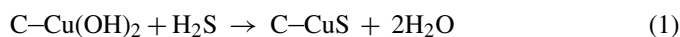


Fig. 4. DTG curves of coconut shell-based AC and IAC. (a) Virgin AC; (b) IAC; (c) IAC after H<sub>2</sub>S adsorption under gas stream without moisture. (Impregnation parameter: pH 3, 0.2 M copper nitrate.)

### 3.4. Reaction mechanism

According to the aforementioned, we assumed the reaction between impregnant supported on the AC and H<sub>2</sub>S as Eq. (1) may be occurred:



The copper species as Cu(OH)<sub>2</sub> loaded onto the porous of AC reacted with H<sub>2</sub>S to form CuS and H<sub>2</sub>O. Except for chemical reaction, the physisorption ability of AC was demonstrated non-exhaustibility by the nitrogen isotherm analysis. Therefore, IAC possessed two parallel ways to adsorb H<sub>2</sub>S, involving both physisorption and chemical reaction.

For a fixed-bed adsorber, the total adsorption capacity of H<sub>2</sub>S was determined by

$$w = F \times Y_{\text{in}} \int_0^{t_s} \left( 1 - \frac{Y_{\text{out}}}{Y_{\text{in}}} \right) dt \quad (2)$$

where  $w$  is the adsorption capacity of H<sub>2</sub>S;  $Y_{\text{in}}$ , the H<sub>2</sub>S concentration at inlet of adsorb-column;  $Y_{\text{out}}$ , the H<sub>2</sub>S concentration at outlet of adsorb-column;  $t$ , the adsorption time (min);  $t_s$ , the saturated time (as  $Y_{\text{out}}/Y_{\text{in}} = 1$ ); and  $F$  is the flow rate (L/min).

Table 3 lists the amount of copper and the adsorption capacity of H<sub>2</sub>S for various coconuts shell based IAC samples. It indicated that the capacity of chemical reaction part was about two times of the amount of copper onto AC. According to Eq.

Table 3  
Adsorption capacity of H<sub>2</sub>S onto coconut shell-based AC and IAC

Impregnation condition	Amount of copper loaded on AC (mmol/g)	Total adsorption capacity (mmol/g)	H <sub>2</sub> S capacity by chemical reaction (mmol/g) <sup>a</sup>
Virgin AC	–	0.127	–
IAC, pH 3, 0.05 M	0.254	0.596	0.469
IAC, pH 3, 0.1 M	0.377	0.872	0.745
IAC, pH 3, 0.2 M	0.625	1.364	1.237

<sup>a</sup> The H<sub>2</sub>S capacity by chemical reaction = (IAC<sub>total capacity</sub> – AC<sub>total capacity</sub>).

(1), the stoichiometric ratio between the impregnant and H<sub>2</sub>S equals to one. Therefore, the reaction as Eq. (1) was not able to explain completely the behavior of chemical reaction part for H<sub>2</sub>S adsorption by IAC.

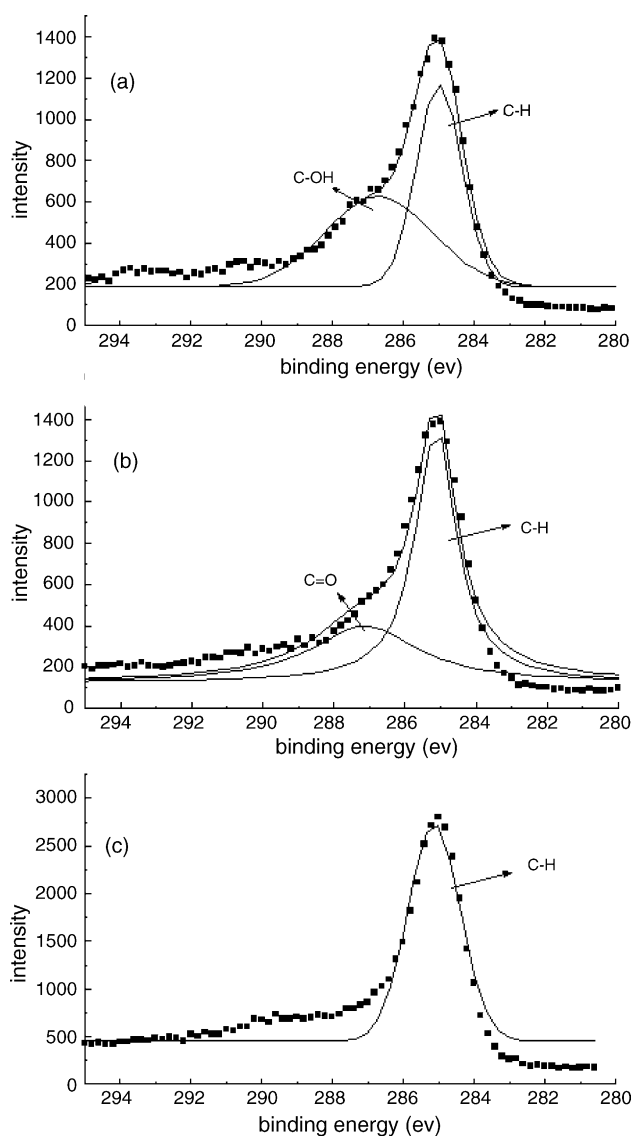
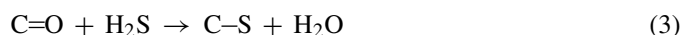


Fig. 5. Detailed C (1s) XPS spectra of coconut shell-based AC and IAC. (a) Virgin AC; (b) IAC; (c) IAC after H<sub>2</sub>S adsorption under gas stream without moisture. (Impregnation parameter: pH 3, 0.2 M copper nitrate.)

Fig. 5 shows the relevant detailed C (1s) XPS spectra of various coconut shell-based AC samples. Generally, these peaks in the curve fitting of C (1s) signal at  $284.8 \pm 0.3$  eV,  $286.3 \pm 0.3$  eV,  $287.6 \pm 0.3$  eV and  $288.8 \pm 0.3$  eV assigned to be C–H, C–OH, C=O and COOH groups, respectively [26]. In this study, it was found that there were significant peaks at 284.9 eV (C–H) and 286.6 eV (C–OH) binding energy site for coconut shell-based AC. After impregnation process, the C–OH groups transferred to C=O groups with binding energy shift to 287.3 eV. Moreover, it was revealed in Fig. 5c that the C=O group disappeared after H<sub>2</sub>S adsorption. Cal et al. [27] proposed that sulfur was adsorbed by carbon–oxygen site to form carbon–sulfur bond in a substitution reaction.



According to above results, the other chemical reaction (as Eq. (3)) might occur during H<sub>2</sub>S adsorption.

### 3.5. Adsorption capacity evaluation

Fig. 6 shows the H<sub>2</sub>S breakthrough curves of the fixed-bed adsorber packed by coconut shell based AC and IAC. The adsorption capacity of H<sub>2</sub>S on the IAC increased with increasing the amount of copper species loaded onto AC. The best adsorption performance of coconut shell based-IAC (impregnation condition: pH 3, 0.2 M) was 10 times larger than that of the virgin coconut shell-based AC. Chiang et al. reported [22] that NaOH-IAC possessed the H<sub>2</sub>S capacity of 0.572 mmol/g. In this study, we obtained the best H<sub>2</sub>S capacity of 1.364 mmol/g using coconut shell-based copper IAC.

### 3.6. Moisture influence

In fact, moisture effect on adsorption capability is important when IAC applies in pollution control. The aging phenomenon

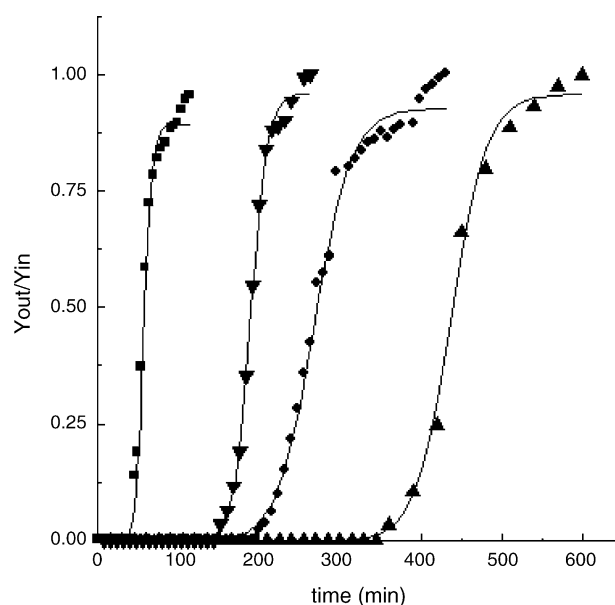


Fig. 6. H<sub>2</sub>S breakthrough curves of coconut shell-based AC and IAC adsorber. (■) Virgin AC; (▼) pH 3, 0.05 M; (●) pH 3, 0.1 M; (▲) pH 3, 0.2 M.



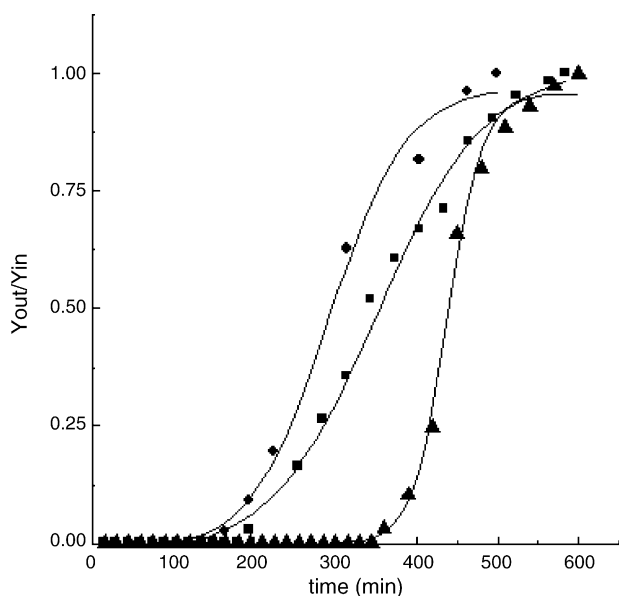


Fig. 7. H<sub>2</sub>S breakthrough curves of coconut shell-based IAC (pH 3, 0.2 M copper nitrate impregnated) under various moisture conditions. (▲) Dry gas stream; (■) gas stream containing RH = 40–50%; (●) gas stream containing RH = 70–80%.

of copper species onto the IAC might be occurred under humid atmosphere. In this study, we conducted two IAC humidification conditions to find out the moisture effect. The H<sub>2</sub>S adsorption capability of IAC for moisture effect discussion was based on the “breakthrough time”. The “breakthrough time” is defined as the time that 1% of H<sub>2</sub>S feed concentration was detected at the outlet of the adsorb-column.

Fig. 7 shows the H<sub>2</sub>S breakthrough curves of coconut shell-based IAC under the gas stream with different RH. The breakthrough times of coconut shell-based IAC for H<sub>2</sub>S removal were collected in Table 4. As expected, it was found from both Fig. 7 and Table 4 that the presence of moisture in the gas stream significantly affected H<sub>2</sub>S adsorption capability of IAC. For instance, the breakthrough time of coconut shell-based IAC (impregnation condition: pH 3, 0.2 M copper nitrate solution) decreased considerably from 350.1 to 156.8 min as the RH of gas stream

increased up to 70–80%. The reasons could be attributed by both physic-sorption and chemi-sorption view points. The competition adsorption between H<sub>2</sub>S and water onto IAC might occur when the moisture existed in the gas stream. According to the Le Chatelier’s principle, both reactions of Eqs. (1) and (3) would be unfavorable to proceed whenever water exists on the IAC. It was also found from Table 4 that the breakthrough time for the pre-moistened case decreased slightly, compared to that for gas stream containing moisture case. From these results, two IAC humidification conditions caused to the discrepancy of adsorption behaviors. The H<sub>2</sub>S adsorption by copper IAC is an exothermic reaction. For gas stream containing moisture case, water vapor was difficult to condense as water film onto the AC during adsorption process. Consequently, both water vapor and H<sub>2</sub>S co-exist and competition adsorption process maybe occurred. For pre-moistened case, IAC was moistened under different RH condition (RH = 40–50% or 70–80%) at 323 K for 24 h. And then, temperature cooling down to room temperature, the absorbed water vapor condensed to be water film in the pores of IAC. Some previous reports [8,23] proposed that the H<sub>2</sub>S dissolved and dissociated to produce H<sup>+</sup> and HS<sup>-</sup> ions into the water film. Therefore, the absorption of H<sub>2</sub>S into water film increased the adsorption capability of the pre-moistened IAC. Additionally, in order to get better understanding about moisture effect, the IAC sample was conducted by pre-moistened in different RH chambers and then dried to remove the condensed water from IAC. The as-prepared IAC finally used to adsorb H<sub>2</sub>S in dry gas stream. The experimental results exhibited that the breakthrough time reduced remarkably as the same shown in gas stream containing moisture cases (see Table 4). The water film was evaporated from IAC after it was dried. Therefore, there was no absorption occurred. Owing to dry gas stream, there was no competition adsorption, either. But, why does the adsorption capability of IAC after aging reduce remarkably?

Ehrburger et al. [28] reported that the copper impregnated onto activated carbon is mainly amorphous copper oxide (CuO). After aging treatment, the amorphous copper oxide may reduce to Cu<sub>2</sub>O or form to crystallization of CuO. McIntyre et al. [25] demonstrated that Cu(I) compounds present on outer surface

Table 4  
Breakthrough time of IAC under various humid conditions

Humid condition	Coconut shell-based IAC (Impregnation condition: pH 3, 0.05 M copper nitrate solution)	Coconut shell-based IAC (Impregnation condition: pH 3, 0.1 M copper nitrate solution)	Coconut shell-based IAC (Impregnation condition: pH 3, 0.2 M copper nitrate solution)
Gas stream without moisture			
IAC	143.7	196.0	350.1
IAC pre-moistened under various RH			
RH = 40–50%	–	142.5	306.4
RH = 70–80%	142.5	175.5	310.1
IAC pre-moistened under various RH and then dried			
RH = 40–50%	107.5	–	196.8
RH = 70–80%	97.5	–	183.7
Gas stream containing moisture			
RH = 40–50%	110.0	84.5	185.7
RH = 70–80%	97.5	52.5	156.8

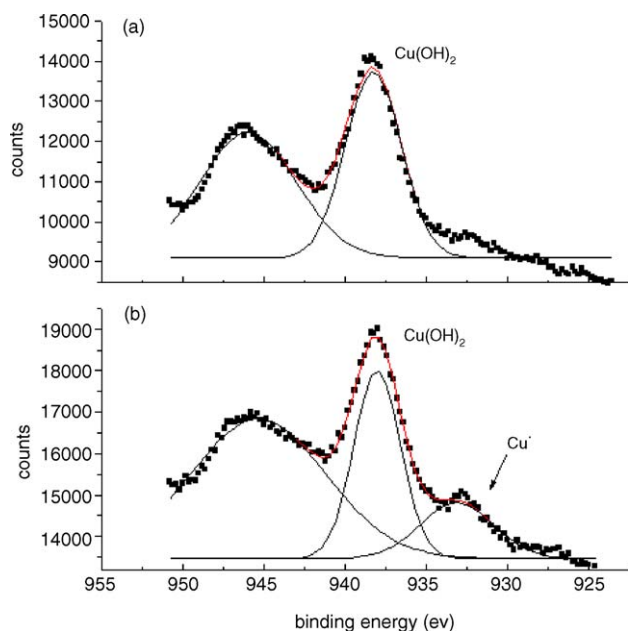


Fig. 8. Detailed Cu(2P<sub>3/2</sub>) XPS spectra of coconut shell-based IAC. (a) Dry IAC; (b) IAC pre-moistened under RH = 40–50% for 24 h. (Impregnation parameters: pH 3, 0.2 M copper nitrate.)

of whetlerite impregnated charcoal became CuO or Cu(OH)<sub>2</sub> after aging. In this study, the curve fittings of the Cu(2P<sub>3/2</sub>) XPS signals for IAC at both dry and pre-moistened conditions were shown in Fig. 8. The main peak with binding energy at  $934.5 \pm 0.3$  eV was assigned to be Cu(OH)<sub>2</sub>. After pre-moistened aging, an extra-peak with binding energy at  $932.5 \pm 0.3$  eV was observed, it was assigned to be Cu(I) species. Part of Cu(II) species on IAC was reduced to Cu(I) species after moisture aging. The effect of moisture on H<sub>2</sub>S adsorption by IAC was obviously negative due to the IAC deactivation.

The total adsorption capacity of H<sub>2</sub>S was also determined by using elemental analysis (EA). As shown in Table 5, it was revealed that the sulfur content of coconut shell-based IAC for

Table 5  
Sulfur elemental analysis of coconut-shell based IAC under various humid conditions and after H<sub>2</sub>S adsorption

Humid condition	pH 3, 0.05 M	pH 3, 0.1 M	pH 3, 0.2 M
IAC before adsorption	0.12 ± 0.10%	0.10 ± 0.10%	0.06 ± 0.10%
IAC after adsorption in gas stream without moisture	2.91 ± 0.10%	3.60 ± 0.05%	3.90 ± 0.10%
IAC pre-moistened (RH = 40–50%) and after adsorption in gas stream without moisture	1.63 ± 0.15%	2.17 ± 0.15%	4.25 ± 0.10%
IAC pre-moistened (RH = 70–80%) and after adsorption in gas stream without moisture	1.69 ± 0.15%	2.35 ± 0.10%	4.12 ± 0.08%
IAC after adsorption in gas stream containing moisture (RH = 40–50%)	1.50 ± 0.03%	2.38 ± 0.11%	3.16 ± 0.15%
IAC after adsorption in gas stream containing moisture (RH = 70–80%)	1.47 ± 0.10%	2.13 ± 0.07%	2.63 ± 0.05%

pre-moistened case was larger slightly than that for gas stream containing moisture case. It was also found that the H<sub>2</sub>S adsorption capability of IAC impregnated by higher copper nitrate concentration (0.2 M) for pre-moistened case was even larger than that for dry gas stream. We suggested that both Cu(OH)<sub>2</sub> and partial copper nitrate compound deposited onto the surface of IAC during impregnation process. It was well known that copper nitrate compound was a stronger moisture absorber. When more copper nitrate compound existed, the water films might be produced easily onto surface of the IAC to absorb H<sub>2</sub>S.

#### 4. Conclusion

In this study, activated carbon was impregnated by copper nitrate solution via incipient wet impregnation process. For the impregnation mechanism, we suggested that the negative charges onto the surface of AC attracted hydrogen ions leading to the pH value of the impregnant solution increase. Then, Cu(OH)<sub>2</sub> was formed and deposited onto the surface of AC. Moreover, the role of Cu(OH)<sub>2</sub> did not only react with H<sub>2</sub>S, but also as a catalyst to catalyze substitution reaction. Through dynamic adsorption experiments, adsorption capacity of IAC was 10 times larger than that of the virgin AC.

It was found that either the existence of moisture in the gas stream or IAC pre-moistened significantly affected H<sub>2</sub>S adsorption capability of the IAC. The moisture effect on H<sub>2</sub>S adsorption capacity of IAC was attributed to the following causes.

1. The copper(II) species supported on the IAC would be reduced to copper(I) species under moist atmosphere.
2. The competition adsorption occurred when the moisture existed in the H<sub>2</sub>S gas stream.
3. According to Le Chatelier's principle, both reactions of Eqs. (1) and (3) would be unfavorable to proceed whenever water exists on the IAC.
4. The H<sub>2</sub>S adsorption capacity was improved when the water film formed onto the IAC.

#### Acknowledgement

This work was financially supported by the National Science Council, Taiwan, Republic of China, under contract (NSC 89-2214-E-224-005).

#### References

- [1] E. Laperdrix, G. Costentin, O. Saur, J.C. Lavalley, C. Nédéz, S. Savin-Poncet, J. Nougayrède, Selective oxidation of H<sub>2</sub>S over CuO/Al<sub>2</sub>O<sub>3</sub>: identification and role of the sulfurated species formed on the catalyst during the reaction, *J. Catal.* 189 (2000) 63–69.
- [2] L.M.L. Leuch, A. Subrenat, P.L. Cloirec, Hydrogen sulfide adsorption and oxidation onto activated carbon cloths: applications to odorous gaseous emission treatments, *Langmuir* 19 (2003) 10869–10877.
- [3] F. Adib, A. Bagreev, T.J. Bandoz, Effect of pH and surface chemistry on the mechanism of H<sub>2</sub>S removal by activated carbons, *J. Colloid Interface Sci.* 216 (1999) 360–369.
- [4] T.J. Bandoz, Effect of pore structure and surface chemistry of virgin activated carbons on removal of hydrogen sulfide, *Carbon* 37 (1999) 483–491.

- [5] A. Bagreev, F. Adib, T.J. Bandoz, pH of activated carbon surface as an indication of its suitability for H<sub>2</sub>S removal from moist air streams, *Carbon* 39 (2001) 1897–1905.
- [6] V. Meeyoo, D.L. Trimm, Adsorption-reaction processes for the removal of hydrogen sulphide from gas streams, *J. Chem. Tech. Biotechnol.* 68 (1997) 411–416.
- [7] J.J. Choi, M. Hirai, M. Shoda, Catalytic oxidation of hydrogen sulphide by air over an activated carbon fibre, *Appl. Catal. A: Gen.* 79 (1991) 241–248.
- [8] J. Klein, K.D. Henning, Catalytic oxidation of hydrogen sulphide on activated carbons, *Fuel* 63 (1984) 1064–1067.
- [9] M. Steijns, F. Derks, A. Verloop, P. Mars, The mechanism of the catalytic oxidation of hydrogen sulfide II. Kinetics and mechanism of hydrogen sulfide oxidation catalyzed by sulfur, *J. Catal.* 42 (1976) 87–95.
- [10] O.C. Cariaso, P.L. Walker, Oxidation of hydrogen sulfide over microporous carbons, *Carbon* 13 (1975) 233–2390.
- [11] A. Primavera, A. Trovarelli, P. Andreussi, G. Dolcetti, The effect of water in the low-temperature catalytic oxidation of hydrogen sulfide to sulfur over activated carbon, *Appl. Catal. A: Gen.* 173 (1998) 185–192.
- [12] H. Katoh, I. Kuniyoshi, M. Hirai, M. Shoda, Studies of the oxidation mechanism of sulphur-containing gases on wet activated carbon fibre, *Appl. Catal. B: Environ.* 6 (1995) 255–262.
- [13] A. Bagreev, H. Rahman, T.J. Bandoz, Study of regeneration of activated carbons used as H<sub>2</sub>S adsorbents in water treatment plants, *Adv. Environ. Res.* 6 (2002) 303–311.
- [14] A. Bagreev, H. Rahman, T.J. Bandoz, Thermal regeneration of a spent activated carbon previously used as hydrogen sulfide adsorbent, *Carbon* 39 (2001) 1319–1326.
- [15] A. Bagreev, H. Rahman, T.J. Bandoz, Wood-based activated carbon as adsorbents of hydrogen sulfide: a study of adsorption and water regeneration processes, *Ind. Eng. Chem. Res.* 39 (2000) 3849–3855.
- [16] A. Bagreev, H. Rahman, T.J. Bandoz, Study of H<sub>2</sub>S adsorption and water regeneration of spent coconut-based activated carbon, *Environ. Sci. Technol.* 34 (2000) 4587–4592.
- [17] M.P. Cal, B.W. Strickler, A.A. Lizzio, High temperature hydrogen sulfide adsorption on activated carbon: I. effects of gas composition and metal addition, *Carbon* 38 (2000) 1757–1765.
- [18] T.J. Bandoz, A. Bagreev, F. Adib, A. Turk, Unmodified versus caustics-impregnated carbons for control of hydrogen sulfide emissions from sewage treatment plants, *Environ. Sci. Technol.* 34 (2000) 1069–1074.
- [19] C. Shin, K. Kim, B. Choi, Deodorization technology at industrial facilities using impregnated activated carbon fiber, *J. Chem. Eng. Jpn.* 34 (2001) 401–406.
- [20] A. Bagreev, T.J. Bandoz, A role of sodium hydroxide in the process of hydrogen sulfide adsorption/oxidation on caustic-impregnated activated carbons, *Ind. Eng. Chem. Res.* 41 (2002) 672–679.
- [21] T. Nakamura, S. Tanada, N. Kawasaki, T. Hara, J. Fujisawa, K. Shibata, Hydrogen sulfide removal by iron containing activated carbon, *Toxicol. Environ. Chem.* 55 (1996) 279–283.
- [22] H.L. Chiang, J.H. Tsai, C.L. Tsai, Y.C. Hsu, Adsorption characteristics of alkaline activated carbon exemplified by water vapor, H<sub>2</sub>S, and CH<sub>3</sub>SH gas, *Sep. Sci. Technol.* 35 (2000) 903–918.
- [23] R. Yan, D.T. Liang, L. Tsen, J.H. Tay, Kinetics and mechanisms of H<sub>2</sub>S adsorption by alkaline activated carbon, *Environ. Sci. Technol.* 36 (2002) 4460–4466.
- [24] R. Yan, T. Chin, Y.L. Ng, H. Duan, D.T. Liang, J.H. Tay, Influence of surface properties on the mechanism of H<sub>2</sub>S removal by alkaline activated carbons, *Environ. Sci. Technol.* 38 (2004) 316–323.
- [25] N.S. McIntyre, G.R. Mount, T.C. Lipson, R. Humphrey, B. Harrison, S. Liang, J. Pagotto, Surface and microanalytical studies of whetlerite charcoals: 1. Effects of aging, *Carbon* 29 (1991) 1071–1079.
- [26] A.F. Pérez-Cadenas, F.J. Maldonado-Hódar, C. Moreno-Castilla, On the nature of surface of chlorinated activated carbons, *Carbon* 41 (2003) 473–478.
- [27] M.P. Cal, B.W. Strickler, A.A. Lizzio, S.K. Gangwal, High temperature hydrogen sulfide adsorption on activated carbon: II. Effects of gas temperature, gas pressure and sorbent regeneration, *Carbon* 38 (2000) 1767–1774.
- [28] P. Ehrburger, J.M. Henlin, J. Lahaye, Aging of cupric oxide supported on activated carbon, *J. Catal.* 100 (1986) 429–436.